Electrical and optical characteristics of hydrogen-plasma treated ZnO nanoneedles

Jinkyoung Yoo, Won Il Park, and Gyu-Chul Yi

Articles you may be interested in

Pulsed-laser treatment of solution-grown ZnO nanowires in nitrogen: Enhancing in electrical conduction and field emission
J. Appl. Phys. **107**, 024312 (2010); 10.1063/1.3284948

Electrical and optical studies of metal organic chemical vapor deposition grown N-doped ZnO films
J. Vac. Sci. Technol. B **27**, 1705 (2009); 10.1116/1.3110018

Photoluminescence properties of ZnO nanoneedles grown by metal organic chemical vapor deposition
J. Appl. Phys. **104**, 064311 (2008); 10.1063/1.2980335

Enhanced luminescent and electrical properties of hydrogen-plasma ZnO nanorods grown on wafer-scale flexible substrates
Appl. Phys. Lett. **86**, 183103 (2005); 10.1063/1.1904715

Remote hydrogen plasma doping of single crystal ZnO
Appl. Phys. Lett. **84**, 2545 (2004); 10.1063/1.1695440

Electrical and optical characteristics of hydrogen-plasma treated ZnO nanoneedles

Jinkyoung Yoo, Won Il Park, and Gyu-Chul Yi[a]

National CRI Center for Semiconductor Nanorods and Department of Materials Science and Engineering, Pohang University of Science and Technology (POSTECH), San-31 Hyoja-dong, Pohang, Gyeongbuk 790-784, Korea

We report on optical characteristics as well as electron emission of hydrogen-plasma treated ZnO nanoneedle arrays. The nanoneedle arrays were vertically grown on Si substrates using catalyst-free metalorganic chemical vapor deposition and subsequently treated by hydrogen plasma at room temperature. After hydrogen plasma treatment, the field emission characteristic curves of nanoneedle arrays exhibited significantly reduced turn-on field and increased emission current density, and the electrical conductivity was increased. In addition, low temperature photoluminesence (PL) measurements indicate that a neutral-donor bound exciton PL peak intensity was increased by the hydrogen- plasma treatment. These effects of the plasma treatment on the physical properties may be explained in terms of hydrogen doping effect. © *2005 American Vacuum Society.* [DOI: 10.1116/1.2037667]

I. INTRODUCTION

Recently increasing attention has been paid to one-dimensional (1D) semiconductor nanostructures such as nanowires and nanorods. Due to possibilities of both band gap and conductivity controls as well as their high aspect ratios, 1D nanostructures offer great potential as building blocks for nanoscale electronic and photonic device applications. Among many semiconductor nanostructures, ZnO 1D nanostructures have attracted much interest due to their electrical and optical properties besides attractive characteristics of ZnO thin films.[1–5] Especially, ZnO 1D nanostructures have shown excellent and stable field emission characteristics comparable to those of carbon nanotubes.[6–12] However, if the nanostructures are to be exploited for most nano-scale semiconductor device applications, defect and doping controls must be possible over a wide range since the effect of defects on physical properties of nanomaterials increases with decreasing dimension of material.[13,14] As already proven in microelectronics, impurity and native defects generate defect levels in a forbidden band gap of the host material and even low defect concentrations significantly affect electrical and optical properties of the material and device characteristics. Nevertheless, dopings of 1D nanostructures have rarely been investigated to date, presumably due to difficulty in preparation of high purity nanomaterials and limited doping methods.[15] We recently demonstrated preparation of high purity ZnO nanomaterials by catalyst-free metalorganic chemical vapor deposition (MOCVD).[16] Here we report on enhancement of electron emission characteristics of hydrogen-plasma treated ZnO nanoneedles and changes in electrical and optical properties of the nanomaterials.

II. EXPERIMENT

Both as-grown and hydrogen-plasma treated ZnO nanoneedle arrays were prepared on *n*-type Si substrates using the MOCVD system. Diethylzinc and oxygen were the reactants and their flow rates were in the range of 20–100 s and 0.5–5 sccm, respectively. Typical growth temperatures were in the 400–500 °C range. No metal catalyst was coated on the substrates during nanoneedle growth. Details of ZnO nanoneedle growth are reported elsewhere.[16,17] After the growth, ZnO nanoneedle arrays were plasma treated under hydrogen flow using a radio frequency (rf)-plasma generator without additional heating. Two series of samples were prepared at hydrogen flow rates of 100 and 200 sccm. Four samples in each series were grown at the same time in the same reactor and three of them were plasma treated at different plasma powers of 0–70 W.

Field emission characteristic curves of both as-grown and plasma-treated nanoneedle arrays were measured with a two-parallel-plate configuration. Before the measurements were taken, Cu was evaporated on the backside of the samples for a cathode-conducting layer and indium tin oxide (ITO)-coated glass plate was used as an anode. The samples (ZnO nanoneedle arrays grown on Si) and the ITO-coated glass were separated using glass spacers with a 200 μm thickness. The measured electron emission area was 0.3 cm^2. The emission current was measured at various applied voltages from 0.1 to 2 kV with a sweep step of 10 V, and was monitored using a picoammeter. All emission current measurements were performed at room temperature in a high vacuum chamber with a 1×10^{-7} Torr. Reproducible emission characteristic curves were obtained after a high electric field of 2 kV was applied for 10 s in order to stabilize the emission current. The emission characteristics of our samples were reproducible during repeated sweeps over three times. To characterize emission current stability, hydrogen plasma

---

[a]Author to whom correspondence should be addressed; electronic mail: gcyi@postech.ac.kr
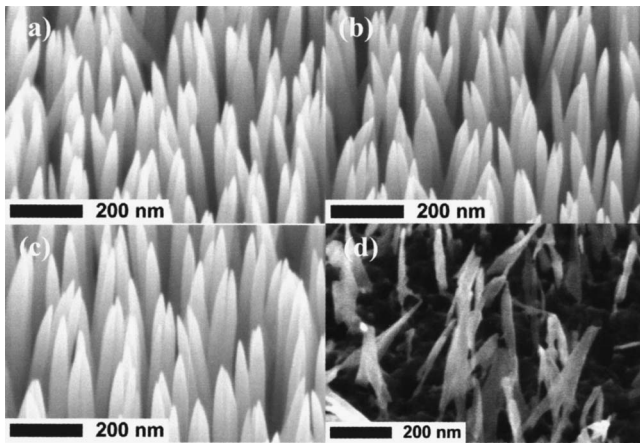
FIG. 1. Electron microscopy images of (a) as-grown and plasma-treated ZnO nanoneedle arrays at a hydrogen flow rate of 200 sccm and rf plasma power of (b) 20, (c) 30, and (d) 50 W. After hydrogen-plasma treatment for the applied plasma power below 30 W, no significant change in morphology of ZnO nanoneedle arrays was observed. For the plasma power higher than 50 W, however, most of the ZnO nanoneedles were etched by hydrogen-plasma treatment.

FIG. 2. I-V characteristic curves of as-grown and plasma-treated ZnO nanoneedle arrays. The I-V characteristic curves show that nanoneedle resistance decreases with increasing plasma power, presumably due to n-type carrier concentration.

treated ZnO nanoneedle arrays with 30 W at a hydrogen flow rate of 100 sccm were kept at applied voltage 1 kV in a high vacuum chamber with a 5×10^{-7} Torr for 1 h.

Tip morphology change of ZnO nanoneedles after hydrogen plasma treatment was investigated using high resolution transmission electron microscope (HRTEM) in order to elucidate the origin of increase in field enhancement factor for hydrogen-plasma treated ZnO nanoneedles.

Changes in electrical and optical properties of ZnO nanoneedles by the hydrogen-plasma treatment were investigated measuring current-voltage (I-V) characteristic curves and photoluminescence (PL) spectra of the samples. Ti/Au contacts were formed on ZnO nanoneedle tips with a thermal evaporator in order to make ohmic contacts for electrical characterization. I-V characteristic curves of the samples were measured at bias voltages applied between the conducting tip and a contact layer in the 0-4 V range with a sweep step of 10 mV. In addition, the PL measurements were performed at 10 K with an optical resolution of 0.05 nm, and the 325 nm line of a continuous wave He–Cd laser was used as the excitation source. Details of PL measurement have been reported previously.[18]

III. RESULTS AND DISCUSSION

Electron microscopy images have revealed the general morphology of vertically well-aligned ZnO nanoneedle arrays before and after the plasma treatment. Figure 1 shows the scanning electron microscopy (SEM) images of as-grown and plasma-treated ZnO nanoneedle arrays at applied rf powers of 20, 30, and 50 W and a pressure of 65 mTorr with a hydrogen flow rate of 200 sccm. As shown in Figs. 1(a)–1(c), no significant change was observed in ZnO nanoneedle array morphology following hydrogen plasma treatment for the applied rf power below 30 W. However, Fig. 1(d) shows that most ZnO nanoneedles were etched by
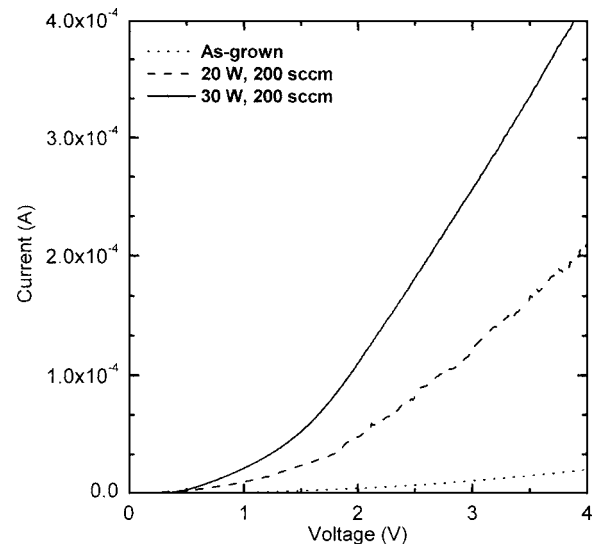
hydrogen-plasma treatment at 50 W, which resulted in destruction of nanoneedle form and deterioration of the vertical alignment of the nanoneedle array. Similar behavior was also observed for samples plasma treated at a pressure of 45 mTorr at a hydrogen flow rate of 100 sccm although the etching occurred at hydrogen plasma powers above 70 W.

An effect of hydrogen-plasma treatment on the electrical characteristics of ZnO nanoneedle arrays was investigated by measuring I-V characteristic curves. Figure 2 shows I-V curves of as-grown and hydrogen-plasma treated ZnO nanoneedle arrays, indicating increase in the current density of ZnO nanoneedle arrays by the hydrogen-plasma treatment. In addition, the resistivity of each ZnO nanoneedle decreased from 6 to 0.6 and 0.3 Ω cm after the hydrogen-plasma treatments at the rf powers of 20 and 30 W, respectively.

Field emission characteristics of as-grown and plasma-treated ZnO nanoneedles were investigated measuring current density emitted at various applied electric fields. Figure 3 shows the emission current characteristic curves of as-grown and hydrogen-plasma treated ZnO nanoneedle arrays at a hydrogen flow rate of 200 sccm. The as-grown ZnO nanoneedle array exhibited a low emission current of $0.02-0.05$ $\mu A/cm^2$ at 10 V/μm, and the turn-on field was not observed up to 10 V/μm. For ZnO nanoneedle arrays plasma-treated at 20 W, however, the turn-on field decreased to 9 V/μm and the emission current at 10 V/μm increased to 0.18 $\mu A/cm^2$. The field emission characteristic was further enhanced for ZnO nanoneedle arrays plasma treated at 30 W: the turn-on voltage and emission current were 3 V/μm and 15 $\mu A/cm^2$, respectively.

Similar behavior was also observed for samples plasma treated at a hydrogen flow rate of 100 sccm. After plasma treatment, sample emission currents were significantly increased and the turn-on field was reduced. As summarized in
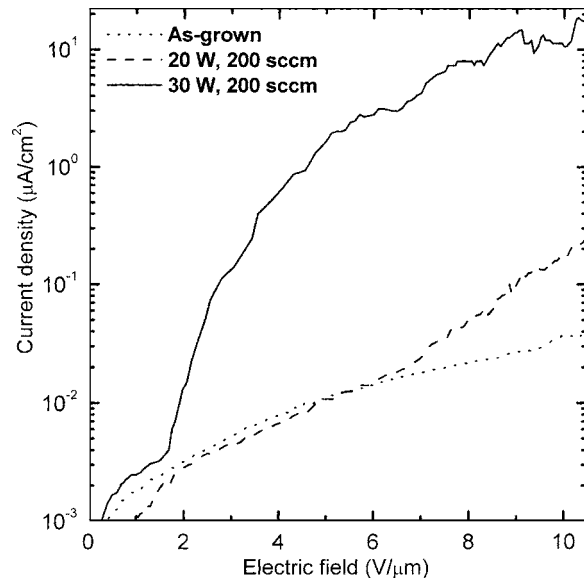
FIG. 3. Field emission characteristic curves of as-grown and plasma-treated ZnO nanoneedle arrays at a hydrogen flow rate of 200 sccm. Although the turn-on field of as-grown ZnO nanoneedle arrays with a criterion of 0.1 $\mu A/cm^2$ emission current density was not observed up to 10 V/μm, the turn-on field of ZnO nanoneedle arrays plasma treated at 20 and 30 W reduces to 9 and 3 V/μm, respectively. In addition, the emission current density was significantly increased by plasma treatment.

Table I, the turn-on field decreased to 11 and 5.2 V/μm after plasma treatment at 20 and 50 W, respectively. However, the turn-on field of ZnO nanoneedle arrays plasma treated at 70 W increased to 8.2 V/μm, presumably due to a hydrogen plasma etching effect at high power. These results indicate that there is an optimum condition in hydrogen plasma treatment for enhancement of field emission characteristics.

In general, field emission current density as a function of applied electric field is fitted using the Fowler–Nordheim equation[19]

$$J = A(\beta^2 V^2/\phi d^2)\exp(-B\phi^{3/2}d/\beta V),$$

where J is the current density, $A = e^3/8\pi ht^2(\Delta\phi/\phi) = 1.56 \times 10^{-10}(AV^{-2}\ eV)$, $B = 6.83 \times 10^9(eV^{-3/2}\ Vm^{-1})$, β a field enhancement factor, ϕ the work function (5.4 eV) of ZnO, $E(=V/d)$ the macroscopic applied electric field, d a distance between the anode and the cathode (a thickness of the glass
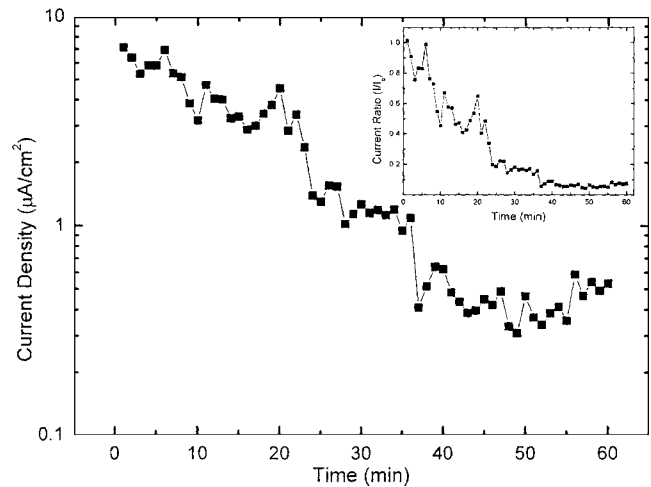

FIG. 4. Field emission current density stability of ZnO nanoneedle arrays treated at 30 W in ahydrogen flow rate of 200 sccm measured at a voltage of 1 kV.

spacers), and V the applied voltage. The field enhancement factor of as-grown ZnO nanoneedle arrays was determined to be in the range of 100–1000 from a slope of the Fowler–Nordheim plot. For ZnO nanoneedle arrays plasma treated at a hydrogen flow rate of 200 sccm, however, plasma treatment resulted in increasing the field enhancement factor to 1600 and 9600 for the rf power of 20 and 30 W, respectively. Similarly, the field enhancement factor increased for the hydrogen plasma treatment at a hydrogen flow rate of 100 sccm. This result indicates that hydrogen plasma treatment induces remarkable enhancement in field emission characteristics of ZnO nanoneedles.

Figure 4 shows field emission current stability as an important prerequisite for useful field emitters. The emission current stability of hydrogen plasma-treated ZnO nanoneedle arrays showed slow decrease and was saturated after about 35 min. The decrease in emission current is not caused by morphological change of ZnO nanoneedle arrays because we could not observe any collapse of ZnO nanoneedle arrays from SEM observation (not shown) of hydrogen plasma-treated ZnO nanoneedle arrays after field emission measurement. The origin of the decrease in the emission current is still under investigation.

TABLE I. Field emission characteristics of as-grown and plasma-treated ZnO nanoneedles.

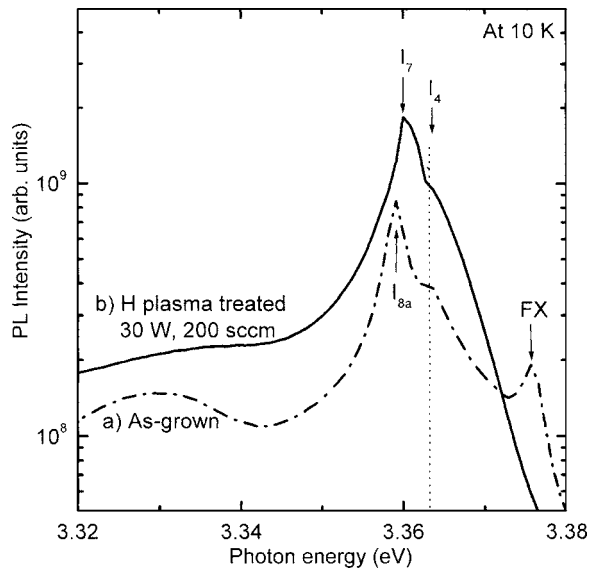| Sample name	Hydrogen flow rate (sccm)	Plasma power (W)	Turn-on field (V/μm) at 1 $\mu A/cm^2$	Emission current density ($\mu A/cm^2$) at 10 V/μm	Field enhancement factor (β)
P390	100	0	>13	0.05	760
		20	11	0.08	1700
		50	5.2	12	4700
		70	8.2	6	2000
P494	200	0	>13	0.02	160
		20	9	0.18	1600
		30	3	15	9600

FIG. 5. Low temperature PL spectra of (a) as-grown and (b) hydrogen-plasma-treated ZnO nanoneedle array. The hydrogen-plasma treatment was performed at the plasma power of 30 W. A dominant PL peak was observed at 3.360–3.365 eV, attributing to neutral donor bound excitons. The PL peak intensity was significantly increased by the hydrogen-plasma treatment.

One possible origin for these enhanced field emission characteristics and electrical conductivity by posthydrogen-plasma treatment may be explained in terms of hydrogen doping into the nanoneedles during the process. The hydrogen doping effect was also investigated measuring low temperature (10 K) PL spectra of ZnO nanoneedle array before and after hydrogen-plasma treatment. As shown in Fig. 5, the PL spectra of the plasma-treated nanoneedles showed significant increases in neutral-donor-bound-exciton peak intensities in the range of 3.360 and 3.365 eV including I_4 line (3.3628 eV) assigned its chemical identity as hydrogen.[20] This behavior is consistent with previous reports that the hydrogen is a shallow level impurity in ZnO, strongly suggesting that hydrogen-plasma treatment increases conductivity of ZnO nanoneedles due to hydrogen doping.[21,22] Meanwhile, high conductivity resulting from high carrier concentrations is one of the most important factors for obtaining excellent field emission characteristics in other materials.[23,24] Hence, we strongly suggest that the enhanced field emission characteristics of ZnO nanoneedles after hydrogen plasma treatment result from the increased carrier concentration due to hydrogen doping.

It is also noted that there may be another possible origin for the enhanced field emission characteristics: a change in geometrical factors such as aspect ratio and tip curvature by hydrogen-plasma treatment.[25] This suggestion is strongly supported by significant increase in the field enhancement factor directly related to the geometrical factors after hydrogen-plasma treatment. However, as shown in Fig. 6, significant difference in tip morphologies after hydrogen-plasma treatment was not observed.
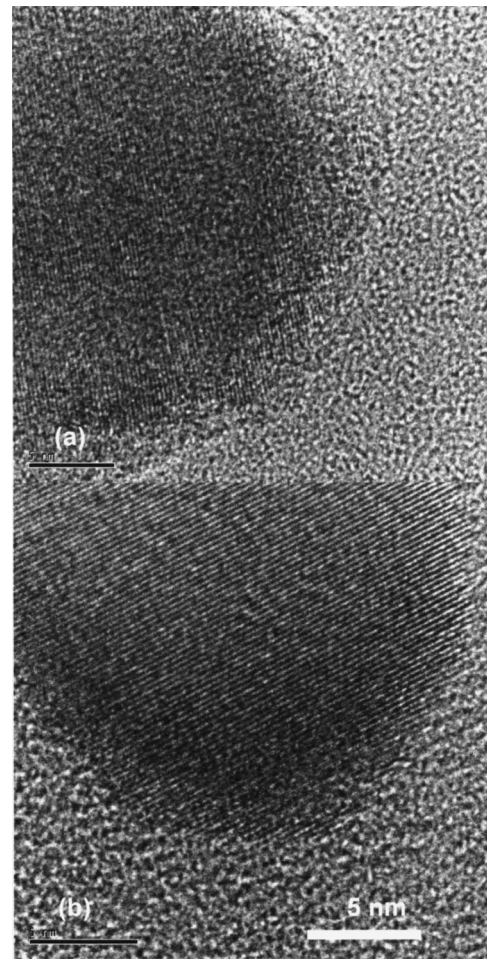

FIG. 6. HRTEM images of (a) as-grown and (b) hydrogen-plasma-treated ZnO nanoneedles. The HRTEM images indicate that hydrogen-plasma treatment did not significantly change tip morphology of ZnO nanoneedles.

IV. CONCLUSION

Our controlled hydrogen-plasma treatment opens up significant opportunities for the fabrication of oxide-based nanodevices based on hydrogen-doped nanomaterials since plasma treatment facilitates effective hydrogen doping in ZnO nanostructures. Hydrogen-plasma treatment increases conductivity of ZnO nanostructures and donor bound exciton PL intensity, implying that hydrogen in ZnO acts as a shallow donor. In particular, enhanced field emission characteristics were observed for hydrogen-plasma treated ZnO nanoneedles presumably due to the increased conductivity. More generally, we believe that simple hydrogen-plasma treatment might readily be expanded to change electrical and optical properties of many other semiconductor nanomaterials.

ACKNOWLEDGMENT

[1] M. H. Huang, S. Mao, H. Feick, H. Q. Yan, Y. Y. Wu, H. Kind, E. Weber, R. Russo, and P. D. Yang, Science **292**, 1897 (2001).

[2] S. F. Yu, C. Yuen, S. P. Lau, W. I. Park, and G.-C. Yi, Appl. Phys. Lett. **84**, 3241 (2004).

[3] Y. Zhang, H. B. Jia, R. M. Wang, C. P. Chen, X. H. Luo, D. P. Yu, and C. J. Lee, Appl. Phys. Lett. **83**, 4631 (2003).

[4] S. Y. Bae, H. W. Seo, and J. Park, J. Phys. Chem. B **108**, 5206 (2004).

[5] X. Feng, L. Feng, M. Jin, J. Zhai, L. Jiang, and D. Zhu, J. Am. Chem. Soc. **126**, 62 (2004).

[6] C. J. Lee, T. J. Lee, S. C. Lyu, Y. Zhang, H. Ruh, and H. J. Lee, Appl. Phys. Lett. **81**, 3648 (2002).

[7] L. Dong, J. Jiao, D. W. Tuggle, J. M. Petty, S. A. Elliff, and M. Coulter, Appl. Phys. Lett. **82**, 1096 (2003).

[8] Y. W. Zhu, H. Z. Zhang, X. C. Sun, S. Q. Feng, J. Xu, Q. Zhao, B. Xiang, R. M. Wang, and D. P. Yu, Appl. Phys. Lett. **83**, 144 (2003).

[9] Q. Wan, K. Yu, T. H. Wang, and C. L. Lin, Appl. Phys. Lett. **83**, 2253 (2003).

[10] S. Y. Jo, J. Y. Lao, Z. F. Ren, R. A. Farrer, T. Baldacchini, and J. T. Fourkas, Appl. Phys. Lett. **83**, 4821 (2003).

[11] S. Y. Li, P. Lin, C. Y. Lee, and T. Y. Tseng, J. Appl. Phys. **95**, 3711 (2004).

[12] J. B. Cui, C. P. Daghilan, U. J. Gibson, R. Püsche, P. Geithner, and L. Ley, J. Appl. Phys. **97**, 044315 (2005).

[13] H. L. Tuller, Electrochim. Acta **48**, 2879 (2003).

[14] H. Gleiter, Met. & Mater Int. **7**, 421 (2001).

[15] C. X. Xu, X. W. Sun, and B. J. Chen, Appl. Phys. Lett. **84**, 1540 (2004).

[16] W. I. Park, G.-C. Yi, M. Kim, and S. J. Pennycook, Adv. Mater. (Weinheim, Ger.) **14**, 1841 (2002).

[17] W. I. Park, D. H. Kim, S. W. Jung, and G.-C. Yi, Appl. Phys. Lett. **80**, 4232 (2002).

[18] W. I. Park, Y. H. Jun, S. W. Jung, and G.-C. Yi, Appl. Phys. Lett. **82**, 964 (2003).

[19] D. Temple, Mater. Sci. Eng., R. **24**, 185 (1999).

[20] B. K. Meyer, H. Alves, D. M. Hofmann, W. Kriegseis, D. Forster, F. Bertram, J. Christen, A. Hoffmann, M. Strßburg, M. Dworzak, U. Haboeck, and A. V. Rodina, Phys. Status Solidi **241**, 231 (2004).

[21] C. G. Van de Walle, Phys. Rev. Lett. **85**, 1012 (2000).

[22] J.-M. Lee, K.-K. Kim, S.-J. Park, and W.-K. Choi, Appl. Phys. Lett. **78**, 3842 (2001).

[23] T. Sugino, K. Kuriyama, C. Kimura, Y. Yokota, S. Kawasaki, and J. Shirafuji, J. Appl. Phys. **86**, 4635 (1999).

[24] M. C. Kan, J. L. Huang, J. C. Sung, K. H. Chen, and D. F. Lii, J. Mater. Res. **18**, 1594 (2003).

[25] Y. B. Li, Y. Bando, and D. Goldberg, Appl. Phys. Lett. **84**, 3603 (2004).